

# **MODELING OF RANDOM FIBER COMPOSITES FOR ENERGY ABSORPTION**

Haeng-Ki Lee<sup>a</sup>, Srdan Simunovic<sup>b</sup>

<sup>a</sup>Department of Civil, Architectural, and Environmental Engineering  
University of Miami, Coral Gables, FL 33124-0620

<sup>b</sup>Computer Science and Mathematics Division  
Oak Ridge National Laboratory, Oak Ridge, TN 37831-6359

## **ABSTRACT**

A computational approach to simulate the crushing behavior of random fiber composites is presented. Material damages induced by fiber debonding and crack nucleation and growth are considered. Systematic computational algorithms are developed to combine micromechanics and continuum mechanics based damage models into the constitutive relation. Based on the computational algorithms, crushing behavior of composite tube is simulated, which shows the applicability of the proposed computational tool for crashworthiness simulations.

**KEYWORDS:** Advanced Composites, Fiber Debonding and Crack Nucleation and Growth, Energy Absorption

## **1. INTRODUCTION**

Random fiber composites are being used increasingly as structural components in aerospace, infrastructure and automotive applications, due to rapid advances in processing science and engineering. These materials have desirable engineering properties (e.g., high strength and stiffness, low density, and high damage tolerance) and can be tailored to meet the intended function of the component. The success of the random fiber composites as a mainstream automotive material depends on the development of high-volume, high-reliability and quality, and cost-competitive manufacturing process that results in the material that meets and exceeds current automotive performance standards. Contrary to the conventional metal structures that collapse by buckling and/or folding involving extensive plastic deformation, random fiber composites fail through a sequence of fracture mechanisms.

In brittle composites such as quasi-brittle random fiber composites and concrete, the interfacial microcracks by the debonding of inclusions and the matrix usually form first due to the fact that (1)

the size of interfacial cracks is usually much larger than that of the matrix voids or cracks and (2) the interfacial layer (transition zone) has a poor microstructure that results in a weaker fracture toughness (Mehta and Monteiro [1]). Although the damage for quasi-brittle random fiber composites is governed by a combined mechanisms, such as interfacial debonding between fibers and the matrix and the subsequent crack nucleation and growth, one damage mechanism is dominant compared to the others depending upon the level of load or deformation. At a smaller load level far below the peak stress in the stress-strain curve, the interfacial debonding usually dominates the damage behavior. As the load increases up to the peak load, the subsequent nucleation of microcracks dominates and major cracks will form from the coalescence of microcracks near the peak load. As the number of cracks multiplies and crack-driving force exceeds the fracture toughness of the materials near the peak load, the balance tilts from the crack nucleation to crack growth (Krajcinovic and Vujosevic [2]).

Predictive analytical and numerical tools required to accurately evaluate and design structural components made of random fiber composites do not currently exist. The availability of predictive tools will be extremely helpful in decreasing the design process time and cost by reducing component testing and increasing the simulation accuracy of random fiber composite structures. A numerical program of research is conducted to develop computational algorithms, by implementing the damage models previously proposed by authors into a finite element code, for simulating the damage evolution and crushing behavior of random fiber composites. Material damages induced by the interfacial fiber debonding, and nucleation and growth of microcracks are considered. Debonding on the interface between fibers and the matrix is simulated by using the micromechanical damage model (Lee and Simunovic [3], [4]; Lee [5]) and the subsequent crack nucleation and growth in the matrix is treated in the framework of the continuum damage mechanics (Lee and Simunovic [6]). The composites are assumed to be quasi-brittle and to have isotropic microcrack distribution. It is also assumed that the damage evolution in the composites is gradual and proportional. By using user-supplied material subroutine, the micromechanics and continuum damage mechanics based damage models are incorporated into the nonlinear finite element code DYNA3D. The overall properties of microcracked composites are estimated using the differential scheme. Using the developed computational algorithms, numerical simulations for an automotive structural component under crash load are carried out to probe crushing behavior of the composites.

## 2. DAMAGE MODELS

This section briefly recapitulates the damage models previously proposed by authors.

**2.1 Micromechanics Based Damage Model: Interfacial Debonding Between Fibers and the Matrix** A micromechanics damage constitutive model proposed by Lee and Simunovic [3], [4] and Lee [5] for randomly oriented discontinuous fiber-reinforced composites is employed to model interfacial debonding between fibers and the matrix. In this micromechanics-based damage model, progressive interfacial debonding between fibers and the matrix is considered to influence the overall stress-strain behavior of composites. The debonding of fibers is assumed to be controlled by the stress of the fibers and the statistical behavior of the fiber-matrix interfacial strength in the form of Weibull probability density function. Only a brief outline of the model is presented in this paper and detail descriptions of the model can be found in Lee [5].

Following Lee [5], in the case of aligned chopped fiber composites, the effective elastic stiffness tensor  $\mathbf{C}^*$  can be explicitly derived as

$$\mathbf{C}^* = \mathbf{F}_{ijkl}(\varphi_1, \varphi_2, \varphi_3, \varphi_4, \varphi_5, \varphi_6, \dots) \quad (1)$$

where the definition of fourth-rank tensor  $\tilde{\mathbf{F}}$  is given in Eq. (2) of Lee and Simunovic [3] and the inverse and product of a fourth-rank tensor  $\tilde{\mathbf{F}}$  are given in the appendix of Ju and Chen [7]. The components  $\varphi_1, \dots, \varphi_6$  are given in the appendix of Lee [5]. Since the fiber orientations are three-dimensional even in composite plates that we are trying to model, it is assumed that all fibers and microcracks in the composite are changed from aligned array to three-dimensional random array. The effective elastic moduli of randomly oriented, chopped fiber composites can be obtained by applying the orientational averaging process proposed by Lee and Simunovic [3]. Assuming the uniform distribution of overall strains, the effective elastic stiffness tensor  $\mathbf{C}^*$  in Eq. (1) is averaged over all orientations as

$$\begin{aligned} \langle \mathbf{C}^* \rangle &= \frac{1}{2\pi} \int_0^\pi \int_0^\pi l_{mi} l_{nj} (\mathbf{C}^*)_{mnpq} l_{pk} l_{ql} \sin\theta d\theta d\phi \\ &= \mathcal{C}_1 \delta_{ij} \delta_{kl} + \mathcal{C}_2 (\delta_{ik} \delta_{jl} + \delta_{il} \delta_{jk}) \end{aligned} \quad (2)$$

with

$$\begin{aligned} \mathcal{C}_1 &= \frac{1}{15} [\tau_1 + 5(\tau_3 + \tau_4 + 3\tau_5)] \\ \mathcal{C}_2 &= \frac{1}{15} [\tau_1 + 10\tau_2 + 15\tau_6] \end{aligned} \quad (3)$$

where  $l_{ij}$  denotes the directional cosine between  $i$ -th primed and  $j$ -th unprimed axes. More detail of the orientational process can be found in Lee and Simunovic [3].

Using the Weibull function, the current partially debonded (damaged) fiber volume fraction  $\varphi_2$  can be obtained as

$$\varphi_2 = \varphi \cdot P_d[(\bar{\sigma}_f)_m] = \varphi \cdot \left\{ 1 - \exp \left[ - \left( \frac{(\bar{\sigma}_f)_m}{S_o} \right)^M \right] \right\} \quad (4)$$

where the hydrostatic tensile stresses of the fibers  $(\bar{\sigma}_f)_m = [(\bar{\sigma}_{11})_f + (\bar{\sigma}_{22})_f + (\bar{\sigma}_{33})_f]/3$ . The constants  $S_o$  and  $M$  in Eq. (4) are scale (Weibull modulus) and shape parameters of the Weibull function, respectively, and  $\varphi$  is the original fiber volume fraction.

**2.2 Continuum Mechanics Based Damage Model: Crack Nucleation and Growth** The model derivation in this subsection is identical to the model by Lee and Simunovic [6] and is here repeated for completeness of the proposed numerical model. The basic assumption of the continuum mechanics based damage model is that the damaged state of a solid can be described by the number of microcracks per unit volume  $N$  and the average size  $\bar{c}$  of microcracks. The constitutive relation for the composites with microcracks distributed in a statistically uniform manner can be expressed as

$$\sigma = C(N, \bar{c}) : \epsilon \quad (5)$$

where “:” denotes the tensor contraction,  $\sigma$  is the macroscopic stress,  $C$  is the overall elasticity tensor,  $\epsilon$  is the macroscopic strain,  $N$  is the number of cracks in composites, and  $\bar{c}$  is the mean crack radius. The derivative of the constitutive equation  $\sigma$  with respect to time  $t$  is called the rate equation for evolving microstructure:

$$\dot{\sigma} = \frac{\partial C}{\partial N} \dot{N} : \epsilon + \frac{\partial C}{\partial \bar{c}} \dot{\bar{c}} : \epsilon + C : \dot{\epsilon} \quad (6)$$

The numerical integration algorithm is employed to integrate the rate equation in Eq. (6) to obtain the overall (macroscopic) stress  $\sigma_{n+1}$  at time  $t=t_{n+1}$  as

$$\sigma_{n+1} = \sigma_n + C : \epsilon_{n+1} + \frac{\partial C}{\partial N} \Delta N_{n+1} : \epsilon_n + \frac{\partial C}{\partial N} \Delta N_{n+1} : \epsilon_{n+1} + \frac{\partial C}{\partial \bar{c}} \Delta \bar{c}_{n+1} : \epsilon_n + \frac{\partial C}{\partial \bar{c}} \Delta \bar{c}_{n+1} : \epsilon_{n+1} \quad (7)$$

Previous investigations on the nucleation of microcracks for several materials have shown that the nucleation rate  $\dot{N}$  of microcracks can be expressed as exponential relations, under the applied stress  $\sigma$ :

$$\dot{N} = \dot{N}_0 \cdot \exp\left\{\frac{\sigma - \sigma_{n0}}{\sigma_1}\right\} \quad \sigma > \sigma_{n0} \quad (8)$$

$$= 0, \quad \sigma \leq \sigma_{n0}$$

where  $\sigma_{n0}$  is the threshold stress for the nucleation of microcracks, and  $\dot{N}_0$  and  $\sigma_1$  are experimentally determined material parameters.

Cracks grow at a fraction of Rayleigh wave speed which for applications is approximated by the shear wave velocity (Addessio and Johnson [8]). The rate of crack growth can be expressed as

$$\dot{\bar{c}} = \sqrt{\frac{E^*}{\rho^*}} \tanh(d_s) \quad (9)$$

where  $E^*$  and  $\rho^*$  are the overall Young's modulus and the density of composites, respectively, and  $d_s$  is the measure of the distance the state of stress exceeds damage surfaces. Damage surfaces that define regions of crack growth can be derived through the volume averaging procedure on instability of individual microcracks. The numerical integration algorithm is needed to integrate the rate equations in Eqs. (8) and (9). By the numerical integration, the continuous time history is discretized into a series of time steps small enough to guarantee that the error introduced by the discretization is within reasonable range. The details of the numerical integration algorithm can be found in Lee and Simunovic [6].

Clearly, it is imperative to construct a general model for the loss of stiffness resulting from the nucleation and growth of microcracks in the composites. The overall elasticity tensor  $C^*$  in Eq. (1) of microcracked composites are estimated using the differential scheme. More details on the overall elastic moduli of composites with microcracks can be found in Lee and Simunovic [6].

### 3. NUMERICAL ALGORITHMS FOR PROGRESSIVE DAMAGE MODELING

The micromechanics and continuum mechanics based damage models are implemented into the explicit finite element code DYNA3D. By writing the subroutines for user supplied materials and incorporating them into the nonlinear finite element program, the progressive damage evolutions due to the interfacial fiber debonding, nucleation of microcracks, and growth of microcracks are taken into account into the constitutive relation for the random fiber composites. The finite element implementation allows us to analyze various numerical tests, to simplify investigation of the effects of modeling variables, and to perform customized post-processing of the data that would be most applicable for this study.

The overall scheme for the user-supplied material subroutines simulating the progressive damage behavior of composite materials for a specified loading or displacement is shown in Figure 1. The algorithm consists of three computational phases denoted by ID, CN, and CG. The ID phase, which is restricted to small strain range ( $\epsilon \leq \epsilon_{limit}$ ; e.g.,  $\epsilon_{limit} = 0.01, 0.015$ ), is related to the micromechanics-based damage model for interfacial debonding between fibers and the matrix, and the CN and CG phases are associated with the continuum damage mechanics based model for crack nucleation and crack growth phases, respectively. The details of the numerical algorithms for the progressive damage modeling can be found in Lee et al. [9]. In the user-material subroutines, history variables, such as the volume fraction of damaged fibers, the number of microcracks, and the mean crack size, are updated at each time increment step.

### 4. SIMULATION OF CRUSHING OF DROP TOWER

The drop tower test has been primarily used as a benchmark to evaluate the capabilities of energy absorption and to investigate crushing behavior of composite materials. A square, chopped carbon/polyurethane composite tube under impact loading is considered to simulate the damage evolution and crushing behavior of the composite tube. Figure 2 shows the finite models for a drop mass, composite tube, and the initiator. In computational model, the drop mass is modeled by a single solid element and the composite tube is modeled by using Belyschko-Tsay shell elements. Nodes on the top edge of composite tube is tied to the bottom of solid element of drop mass. A contact surface is defined between the nodes of composite tube and segments of initiator element face. The initiator is modeled as rigid wall restrained in all degrees of freedom and laid at the bottom.

For the elements that lose their load-carrying capability as the cracks in the elements grow significantly, the element elimination algorithm provided in DYNA3D is applied to avoid numerical difficulties that may be encountered during numerical simulation. An initial velocity of 8.75 m/sec is applied on nodes of composite tube and drop mass. The material properties of the carbon/polyurethane are  $E_m=2.067$  GPa,  $\nu_m=0.35$ ,  $E_f=227.4$  GPa,  $\nu_f=0.23$ ,  $\rho=1,493$  kg/m<sup>3</sup>,  $\sigma^*=213$  GPa,  $\epsilon^*=187$  GPa. The details of values of crack nucleation and growth related parameters used in this simulation can be found in Lee et al. (2002). In the user-material subroutines, history variables such as the mean crack radius are monitored at each time step. It is assumed that the tube is reached to its ultimate failure either by the accumulation of growth of cracks (strain driven failure criterion) or by the excessive stresses (stress driven failure criterion).

Figure 3 shows the sequence of deformed shaped of the square carbon/polyurethane composite tube. First, failure starts from the corner of composite tube. As the corner failure proceeds, the weakest segment of the tube in the other direction is folded. The segment of folded section then fails. Figure 4 shows the predicted force-displacement ( $P-u$ ) curves for the composite tube. After  $P-u$  curves reach peak, they start to fluctuate due to progressive crushing of composite tube. Two failure criteria are employed in the drop tower test simulation: 1) stress driven failure criterion and 2) strain driven failure criterion. Figure 5 exhibits a typical stress-strain curve of softened composites, where point A represents critical point of stress driven failure criterion and point B represents critical point of strain driven failure criterion. In Figure 4, top two curves represent the predicted  $P-u$  curves for strain driven failure criterion. Because of the nature of two different failure criteria, one can observe that tube absorbs more energy when using a strain driven failure criterion.

## 5. CONCLUDING REMARKS

The damage evolution of random fiber composites under crushing type of loading is investigated. Material damages induced by the interfacial fiber debonding, the nucleation of microcracks, and the growth of cracks are considered. The user-supplied material subroutines are coded using the damage models and incorporated into the nonlinear finite element code DYNA3D. Numerical simulation for the crushing behavior of composite tube shows the applicability of the present computational procedure for crashworthiness simulations. The developed damage model includes several model parameters that have to be input in the computer program. Future efforts need to be made to determine the parameters for the calibration of composite constitutive model. Furthermore, experimental crash tests for random fiber composite structures are necessary to verify the present procedure on the crashworthiness simulations.

ACKNOWLEDGEMENTS: This research was sponsored by the U.S. Department of Energy, Assistant Secretary for Energy Efficiency and Renewable Energy, Office of Transportation Technologies, Lightweight Materials Program, under contract DE-AC05-00OR22725 with UT-Battelle, LLC.

The submitted manuscript has been authored by a contractor of the U.S. Government under contract No. DE-AC05-00OR22725. Accordingly, the U.S. Government retains a nonexclusive, royalty-free license to publish or reproduce the published form of this contribution, or allow others to do so, for U.S. Government purposes

## 6. REFERENCES

1. P.K. Mehta and P.J.M. Monteiro, *Concrete: structure, properties, and materials*, Prentice-Hall, Englewood Cliffs, NJ (1993).
2. D. Krajcinovic and M. Vujosevic, *Int. J. Solids Structures*, **35**, 2487 (1998).
3. H.K. Lee and S. Simunovic, *Composites Part B: Engineering*, **31**, 77 (2000).
4. H.K. Lee and S. Simunovic, *Int. J. Solids Structures*, **38**, 875 (2001).
5. H.K. Lee, *Computational Mechanics*, **27**, 504 (2001).
6. H.K. Lee and S. Simunovic, *Int. J. Solids Structures*, submitted.
7. J.W. Ju and T.M. Chen, *Acta Mechanica*, **103**, 123 (1994).
8. F.L. Addessio and J.N. Johnson, *J. Appl. Phys.*, **67**, 3275 (1990).
9. H.K. Lee, S. Simunovic, and D.K. Shin, *Comput. Meth. Appl. Mech. Eng.*, submitted

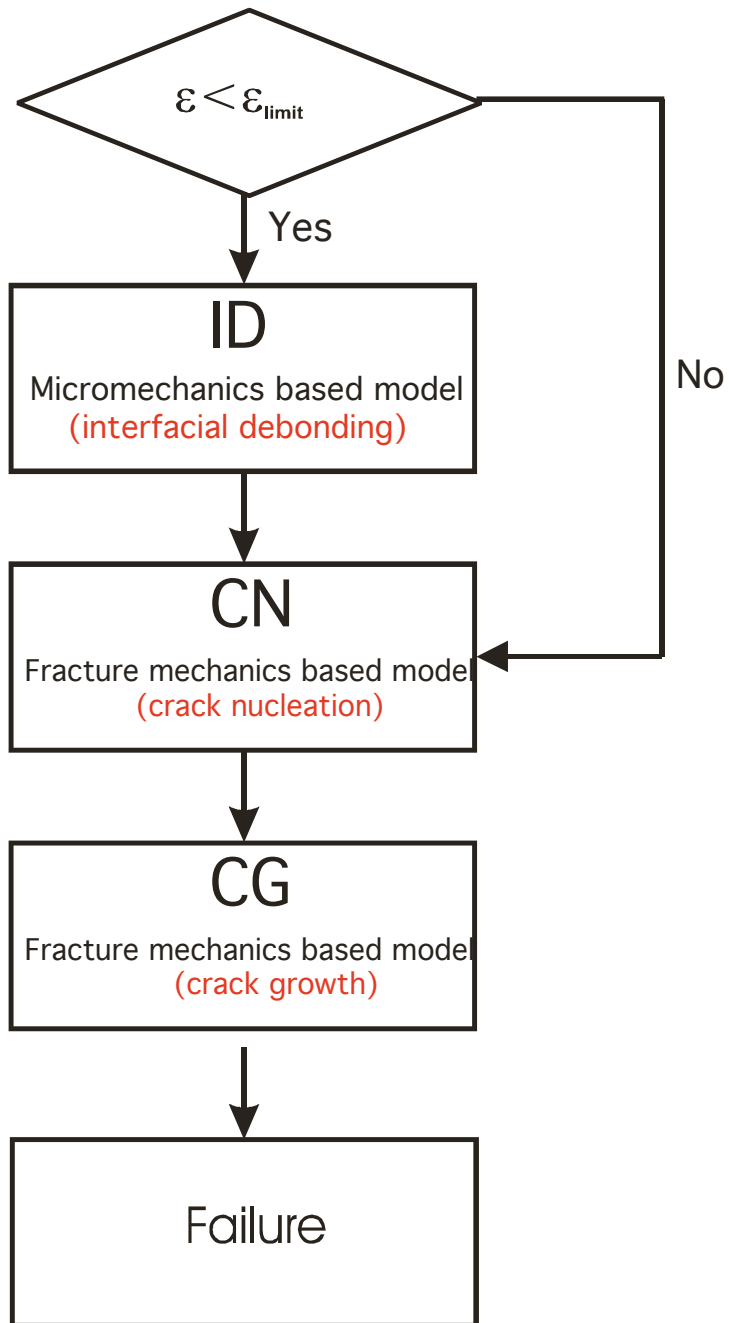


Figure 1. Overall algorithm for user-supplied subroutine.

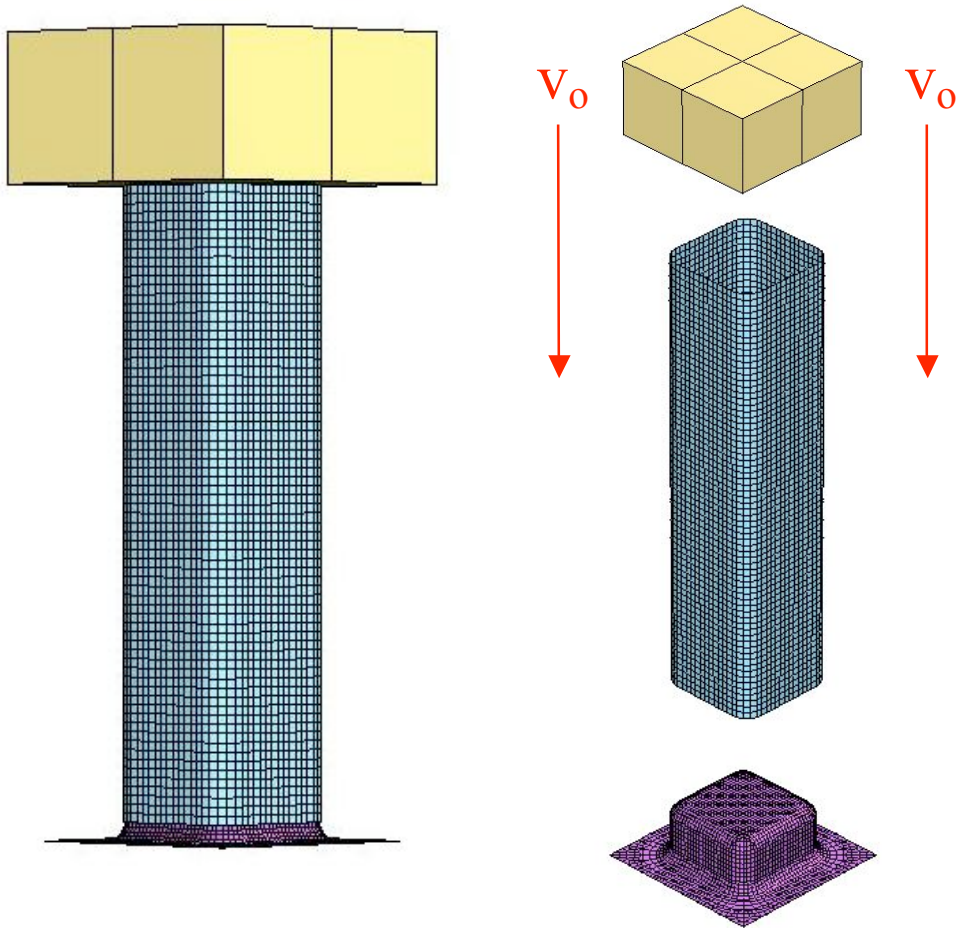
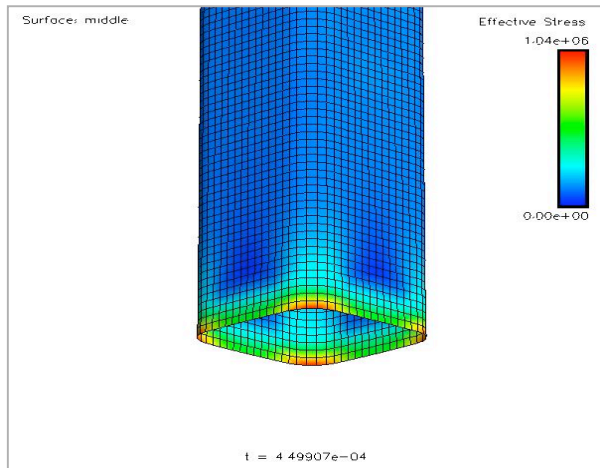
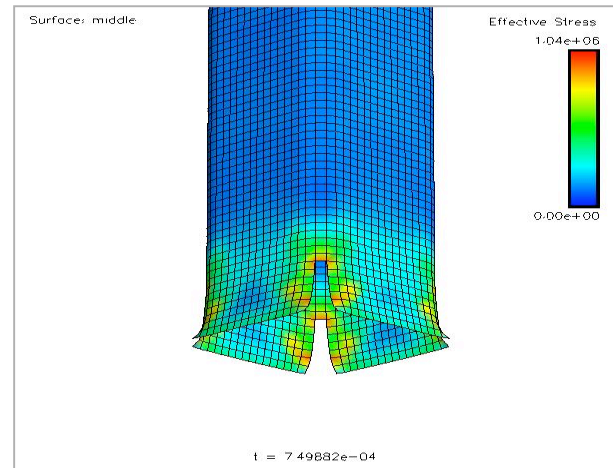


Figure 2. Finite element models for drop tower simulation.

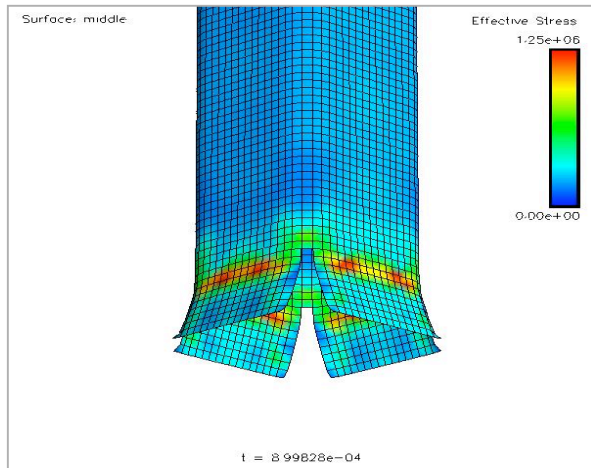


t = 0.45 msec



t = 0.75 msec

t = 0.90 msec



t = 1.65 msec

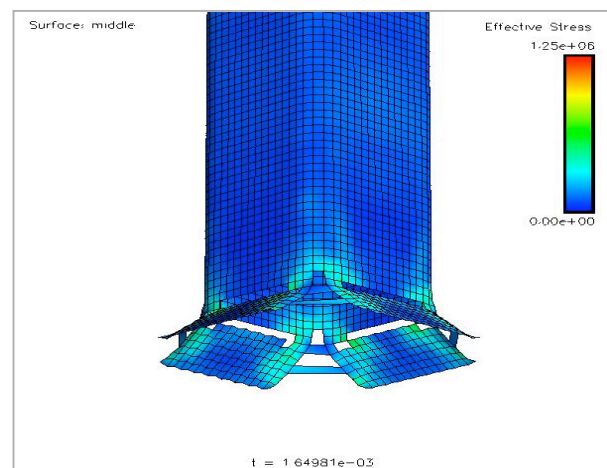


Figure 3. A sequence of deformed shape of the square tube during crushing.

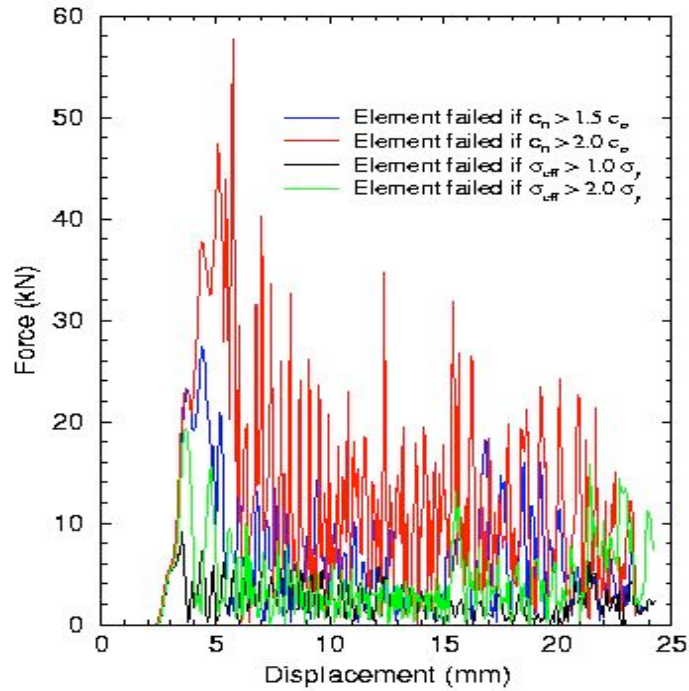


Figure 4. The comparison of force-displacement ( $P-u$ ) curves between two different failure criteria.

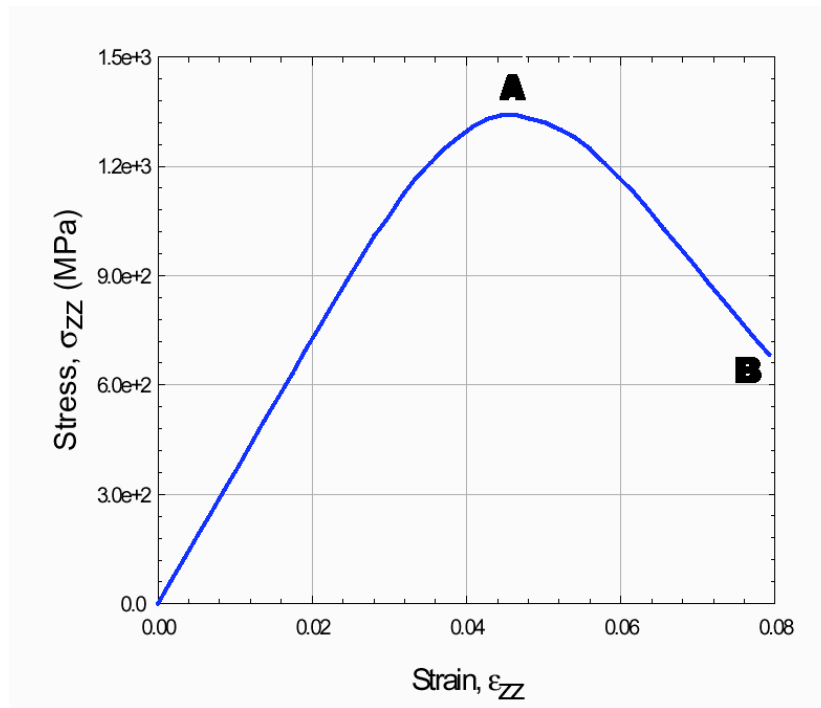


Figure 5. A typical stress-strain curve of softened composites, where A and B represent critical points of stress driven and strain driven failure criteria, respectively.